IEEE Photonics Journal
An IEEE Photonics Society Publication

Open Access

Ultrabroadband Compact Graphene–Silicon TM-Pass Polarizer

Volume 9, Number 2, April 2017

Xiao Hu
Jian Wang

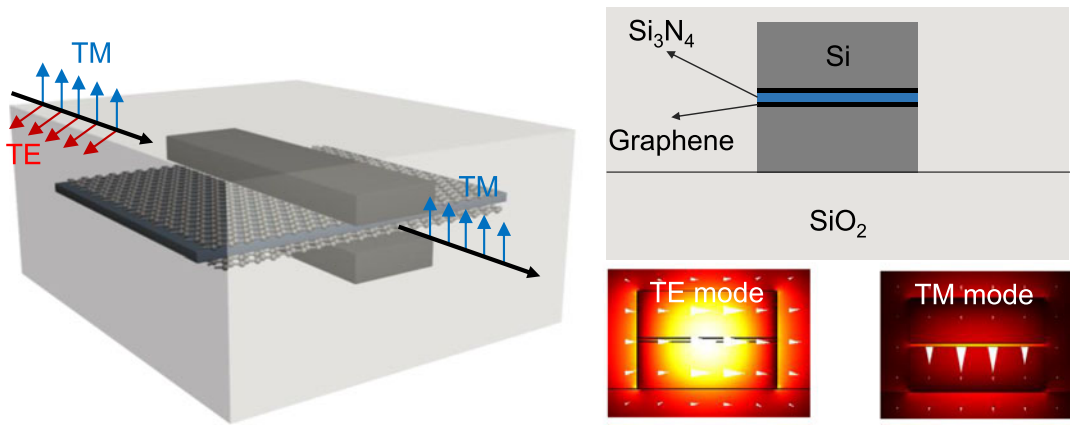

DOI: 10.1109/JPHOT.2017.2672901
1943-0655 © 2017 IEEE

IEEE photonics SOCIETY

IEEE

Ultrabroadband Compact Graphene–Silicon TM-Pass Polarizer

Xiao Hu and Jian Wang

Wuhan National Laboratory for Optoelectronics, School of Optical and Electronic Information, Huazhong University of Science and Technology, Wuhan 430074, China

DOI:10.1109/JPHOT.2017.2672901

Manuscript received January 12, 2017; revised February 14, 2017; accepted February 16, 2017. Date of publication March 1, 2017; date of current version March 14, 2017. This work was supported in part by the National Natural Science Foundation of China under Grant 61222502, Grant 11574001, and Grant 61077051; in part by the Program for New Century Excellent Talents in University under Grant NCET-11-0182; in part by the Wuhan Science and Technology Plan Project under Grant 2014070404010201; in part by the Fundamental Research Funds for the Central Universities under Grant 2012YQ008 and Grant 2013ZZGH003; and in part by the seed project of Wuhan National Laboratory for Optoelectronics.
Corresponding author: J. Wang (e-mail: jwang@hust.edu.cn).

Abstract: Graphene is treated as an anisotropic material because it is one atom thick and its π electrons cause electric conduction in its plane. Based on the polarization-dependent absorption, we design compact broadband transverse-magnetic (TM)-pass polarizer by exploiting a graphene–silicon horizontal slot waveguide structure on silicon-on-insulator (SOI) platforms. The interaction between light and graphene is greatly enhanced by placing the double-layer graphene sheets adjacent to the slot waveguide. The selection of the geometric parameters (e.g., waveguide width, silicon, and Si_3N_4 thicknesses) is discussed. We study the mode properties, extinction ratio (ER), bandwidth, and insertion loss. The graphene–silicon slot waveguide based polarizer offers the performance of high extinction ratio, low insertion loss, broad bandwidth, small footprints, and compatibility with an SOI platform. By employing a 150 μm long graphene–silicon horizontal slot waveguide, the ER is higher than 40 dB, and the insertion loss is less than 3 dB over the 1450–1650 nm wavelength range. We also analyze the impacts of practical fabrication imperfections on the operation performance, i.e., fabrication error tolerance, and give the possible fabrication process of graphene–silicon horizontal slot waveguide based polarizer.

Index Terms: Graphene, silicon photonics, silicon waveguide, slot waveguide, polarizer.

1. Introduction

The silicon-on-insulator (SOI) platform has been widely used for integrated optics in recent years. The compatibility of SOI platform with complementary metal-oxide semiconductor (CMOS) platform indicates the potential combination of electronics and photonics. SOI waveguides can guide light in sub-wavelength scale area due to the high refractive index contrast of silicon (Si) with air or silica (SiO_2), which however makes SOI waveguides highly polarization dependent. Hence, controlling the polarization state is necessary when, for example, connecting a standard optical fiber with light in random polarization state to an SOI chip1. Using a polarizer to eliminate the undesired polarization state is a practical solution. Different schemes of polarizer have been proposed and demonstrated on SOI platforms, such as transverse-electric (TE) and TM-pass polarizer based on hybrid plasmonic waveguide [1]–[3]. These devices might suffer from relatively large insertion loss caused by the intrinsic ohmic loss of metal. Other schemes like TE-pass polarizer using hybrid

plasmonic Bragg grating [4] and TM-pass waveguide polarizer based on slot-induced birefringence [5] have been theoretically proposed.

Graphene, which is a single sheet of carbon atoms in the form of honeycomb lattice, has drawn growing interest because of its alluring electrical and optical properties [6]–[10]. Various significant photonic or electronic devices have been proposed, including modulators [11]–[14], transistors [15], biosensors [16], and ultrafast photodetectors [17]. Among them, a graphene-based waveguide-integrated electro-absorption modulator [11], [12] attracts great attention. The modulation is realized by actively tuning the Fermi level of a monolayer graphene sheet, and the graphene is integrated with a silicon waveguide on an SOI platform, which greatly enhances the light-graphene interaction. Beyond graphene-assisted modulator, the strong electro-absorption effect implies that the graphene-waveguide-integrated structure also has the potential to be used as a polarizer.

Recently, polarizers based on graphene have also been demonstrated. An in-line fiber-to-graphene coupler based TE-pass polarizer [18] achieves an ER up to 27 dB in the telecommunications band. The fabrication of this polarizer is simple and it is based on fiber not SOI platform. Another interesting graphene based polymer waveguide polarizer [19] is planar lightwave circuit (PLC)-type and the length of the device is relatively long (centimeter-scale). More recently, a broadband PLC type graphene/glass hybrid waveguide polarizer with about 4-mm graphene coating length along the propagation direction has been experimentally demonstrated [20]. It is very impressive but also may suffers from large footprint and incompatible with SOI platform. TE-pass polarizer [21] based on multilayer (six-layer) graphene embedded in the silicon slot waveguide is proposed and demonstrated. The chemical potential of graphene should be tuned to 0.49 eV by drive voltage and the graphene is treated as an isotropic material. However, in the work of Min-Suk Kwon [22], he discusses that graphene need to be treated as an anisotropic material and the epsilon-near-zero (ENZ) effect does not exist. Then, the horizontal slot waveguides may not be appropriate for graphene-based polarizers for TE mode. The correct way to design graphene based waveguide polarizers is in-depth discussed in [23]. However, in this work, the optimized TE- or TM-pass polarizers via tuning of the superstrate's index or of the waveguide height suffers from low extinction ratio and large insertion loss as the overlap between the optical mode and the single-layer graphene is relatively small. To mitigate these problems mentioned above, the aim of the work described here is to investigate a polarizer with the performance merits of high ER, low insertion loss, broad bandwidth, small footprints, and compatible with SOI platform.

In this paper, we propose compact broadband TM-pass polarizer on SOI platforms utilizing the electro-absorption effect of graphene. In order to enhance the interaction of graphene with light, we put the double-layer graphene sheet on the slot region of the silicon slot waveguide. We calculate the mode properties of the graphene-silicon slot waveguide and evaluate the ER and bandwidth of the graphene-assisted polarizer.

2. Gate-Variable Dielectric Constant of Graphene

Here, graphene is treated as an anisotropic material because it is one atom thick and its π electrons cause electric conduction in its plane [22]. The out-of plane conductivity $\sigma_\perp$ can be different from the in-plane conductivity $\sigma_\parallel$. For the in-plane optical conductivity $\sigma_\parallel$ of graphene, an analytic expression derived within the random phase approximation [22] is used, which is

$$\sigma_\parallel = \sigma_{\text{inter}} + \sigma_{\text{intra}} = \frac{i8\sigma_0}{\pi}\frac{E_{th}}{E_{ph}+iEs}\ln\left[2\cos\left(\frac{E_F}{2E_{th}}\right)\right] + \sigma_0\left[\frac{1}{2}+\frac{1}{\pi}\tan^{-1}\left(\frac{E_{ph}-2E_F}{2E_{th}}\right)-\frac{i}{2\pi}ln\frac{(E_{ph}+2E_F)^2}{(E_{ph}-2E_F)^2+4E_{th}^2}\right] \quad (1)$$

where $\sigma_0 = e^2/4\hbar$ is the universal conductivity of graphene (e is the charge of an electron, and $\hbar$ is the reduced Planck constant), $E_{th} = k_B T$ is thermal energy in eV ($k_B$is the Boltzmann constant, and T is the temperature), E_F is the Fermi energy (that is chemical potential μ) of graphene in eV,

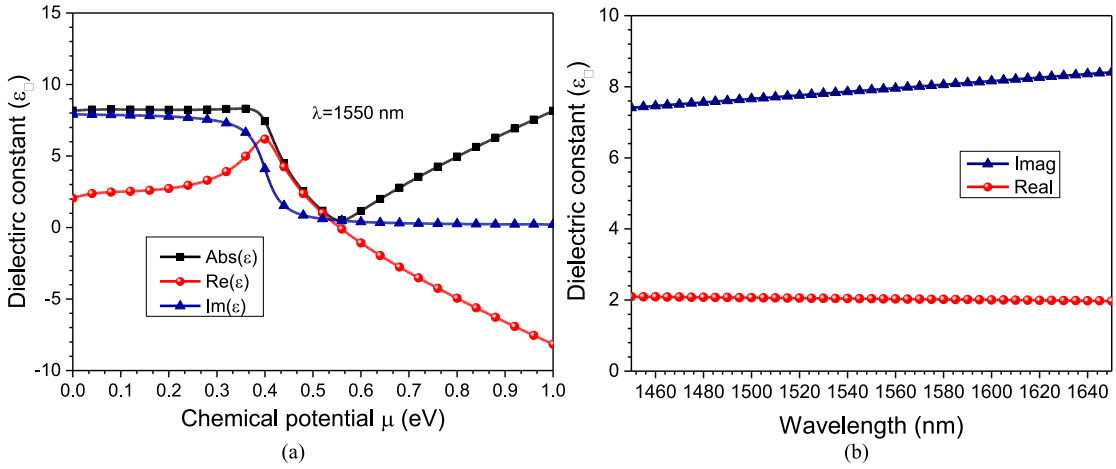

Fig. 1. (a) Calculated dielectric constant of graphene (real part, imaginary part and magnitude) versus chemical potential at $\lambda = 1550$ nm. (b) Permittivity of graphene versus incident light wavelength under chemical potential of graphene $\mu = 0$ eV.

$E_{ph} = hc/\lambda$ is photon energy in eV (h is the Planck constant), and $E_s = \hbar/\tau$ is scattering energy in eV for the scattering time τ.

The complex dielectric function $\varepsilon_{\parallel}(\mu)$can be obtained from the complex optical conductivity of graphene written by

$$\varepsilon_{\parallel}(\mu) = 2.5 + \frac{i\sigma_{\parallel}(\mu)}{\omega\varepsilon_0\Delta} \tag{2}$$

where $\Delta = 0.7$ nm is a thickness of the graphene layer, and $\varepsilon 0$ is the permittivity of vacuum, but the out-of plane permittivity is assumed to be $\varepsilon_{\perp} = 2.5$ [22].

The dielectric constant $\varepsilon_{\parallel}$ of graphene is calculated as a function of the chemical potential μ for a wavelength of $\lambda = 1550$ nm, T = 300 K, $\tau = 0.1$ ps, as shown in Fig. 1(a). Fig. 1(b) shows the dielectric constant of graphene as a function of incident light wavelength when chemical potential of graphene is 0 eV.

3. Design Structure and Principle of the Graphene-Based Silicon Vertical Slot Waveguide Polarizer

The three-dimensional (3D) schematic illustration and cross-section view of graphene-based silicon vertical slot waveguide polarizer and the simulated electric fields of the TE (E_x) and TM (E_y) modes are shown in Fig. 2. The two graphene sheets are sandwiched between the silicon and Si_3N_4 layers. It is expected that the electric field of the TM mode is well guided from the input to the output in the propagation direction, although it suffers the propagation loss. On the contrary, the TE mode experiences rapid attenuation, and therefore cannot propagate through the graphene-waveguide structure (Si/graphene/Si_3N_4/graphene/Si).

The polarizing effect in graphene-waveguide structure is because of the fact that optical absorption in graphene takes place only for the fraction of the electric field which is parallel to graphene's plane. For TM and TE polarized modes, only the corresponding field component has an effective interaction with graphene. Therefore, the mode that presents the higher fraction of its field parallel to graphene, at the graphene position, experiences the higher absorption. In the model of anisotropic graphene, horizontal slot waveguides are not appropriate for absorption of TM mode [22] which is because graphene has an almost real surface-normal dielectric constant component, that is, 2.5. When the double-layer graphene sheets are placed close to the slot region, its interaction with TE mode can be greatly enhanced. Consequentially, the loss of TE mode is very large. While the loss

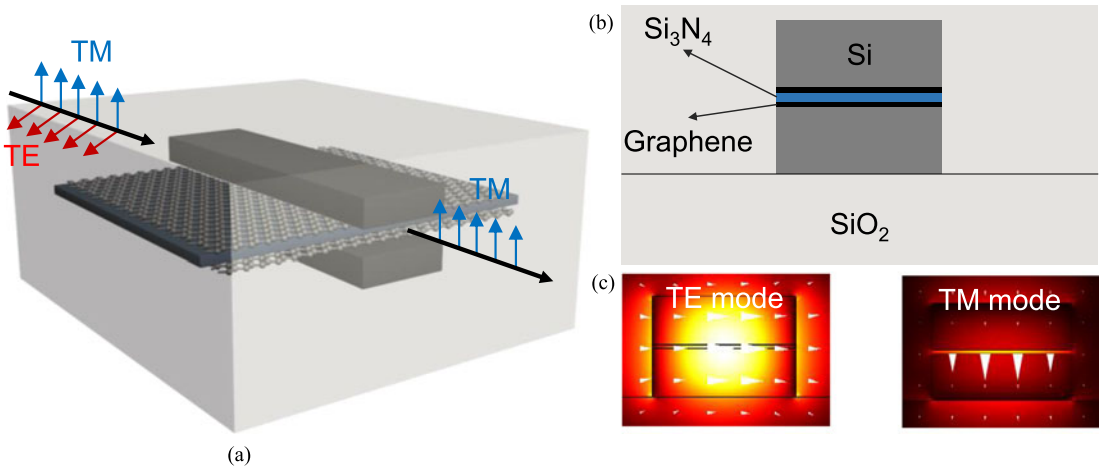

Fig. 2. (a) Three-dimensional schematic illustration of graphene-based polarizer. (b) Cross-section view of the graphene-based polarizer. (c) Electric field (Ex, Ey) distribution of TE and TM mode.

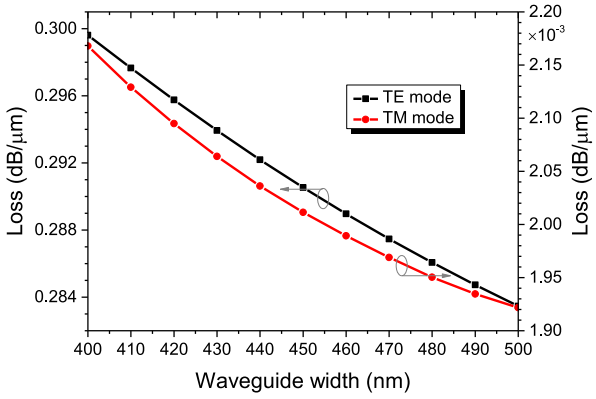

Fig. 3. Loss of TE and TM modes versus waveguide width for the graphene-silicon horizontal slot waveguide based polarizer. The incident light wavelength is 1550 nm.

of TM mode is relatively small. Here, the mode properties of the graphene-assisted waveguide is calculated by the finite element method (FEM) with the scattering bound condition and the simulation domain is surrounded by a rectangular perfectly matched layer (PML). The permittivities of silicon, SiO_2 and Si_3N_4 in 1450 to 1650 nm wavelength range are taken from [24]. For example, the refractive indices of silicon, SiO_2 and Si_3N_4 at 1550 nm are 3.47, 1.45, and 1.98, respectively.

4. Selection of Geometric Parameters of the Graphene-Based Silicon Vertical Slot Waveguide Polarizer

Fig. 3 shows the calculated loss as a function of the waveguide width for the graphene-silicon horizontal slot waveguide based polarizer. The incident light wavelength is 1550 nm. As shown in Fig. 3, for TE mode, the loss varies from 0.299 dB/μm to 0.284 dB/μm when the waveguide width changes from 400 nm to 500 nm (i.e. $\pm$50 nm from 450 nm). For TM mode, the loss varies from 2.17×10^{-3} dB/μm to 1.92×10^{-3} dB/μm. It is obvious that the loss is not sensitive to the change of the waveguide width. We choose a moderate width of 450 nm. In contrast, the loss is relatively sensitive to the change of the Si and Si_3N_4 thickness. As shown in Fig. 4(a), for TE mode, the loss varies from 0.324 dB/μm to 0.229 dB/μm when the Si thickness changes from 130 nm to 180 nm.

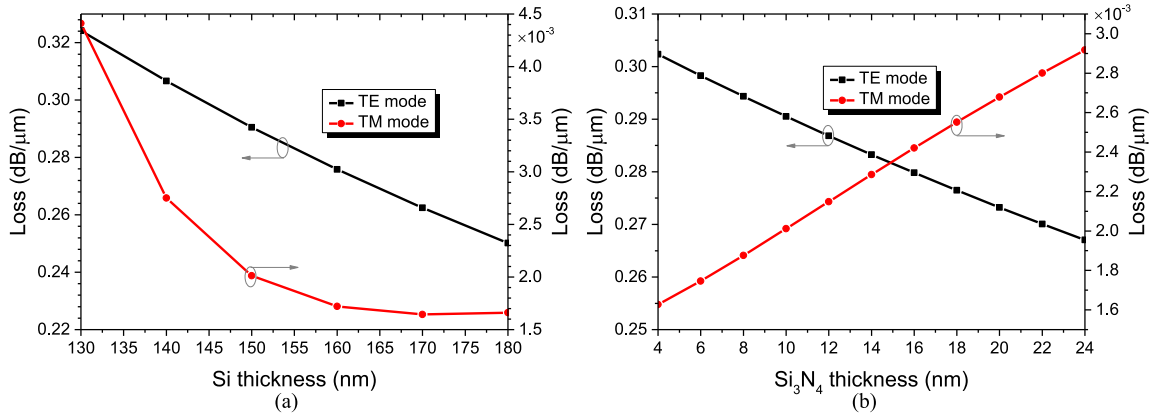

Fig. 4. Loss of TE and TM modes versus (a) Si thickness and (b) Si_3N_4 thickness for the graphene-silicon horizontal slot waveguide based polarizer. The incident light wavelength is 1550 nm.

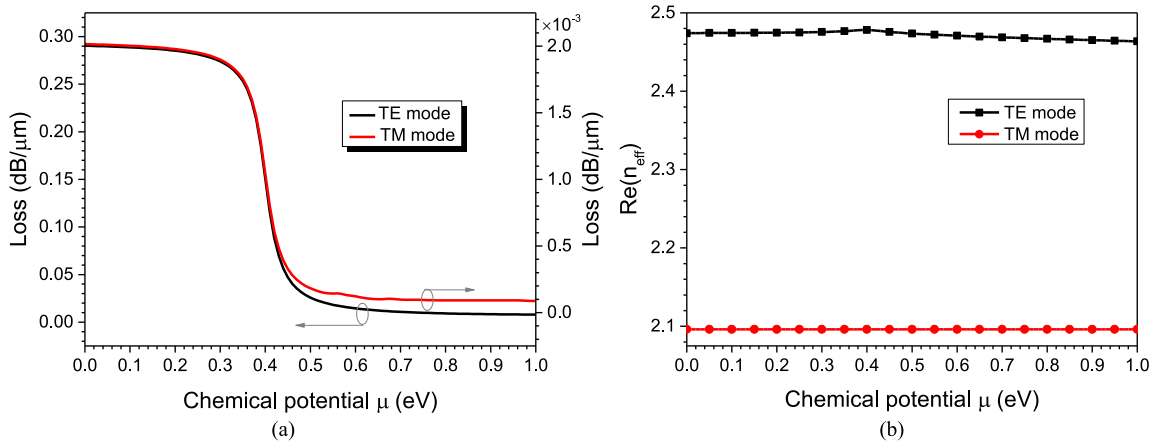

Fig. 5. Loss (a) and real part of effective modal index $Re(n_{eff})$ (b) of graphene-based silicon vertical slot waveguide polarizer versus graphene chemical potential at incident light wavelength $\lambda = 1550$ nm for TE and TM modes.

For TM mode, the loss varies from 4.41×10^{-3} dB/μm to 1.71×10^{-3} dB/μm. The Si film on each side of graphene is set as 150 nm. From Fig. 4(b), one can see that the smaller Si_3N_4 thickness of graphene-silicon horizontal slot waveguide polarizer provides larger loss of TE mode. The Si_3N_4 thickness is set as 10 nm. The thickness of the graphene sheet is modeled as 0.7 nm.

5. Results and Discussions

We first study the chemical potential dependence of loss and the real part of effective modal index $Re(n_{eff})$ for TE and TM modes. After that, we choose the working chemical potential of graphene-based silicon vertical slot waveguide polarizer and define the ER. Then, the ER as a function of the incident light wavelength is evaluated. Finally, we also analyze the fabrication error tolerance.

From Fig. 1(a), it is reminded that the complex dielectric constant of graphene can be tuned by changing the chemical potential of graphene through the applied drive gate voltage. The change of the complex dielectric constant of graphene affects the mode property (e.g. loss and real part of effective modal index $Re(n_{eff})$. In Fig. 5, the simulated loss and real part of effective modal index $Re(n_{eff})$ of the whole structure as a function of the graphene's chemical potential μ (Fermi level) at

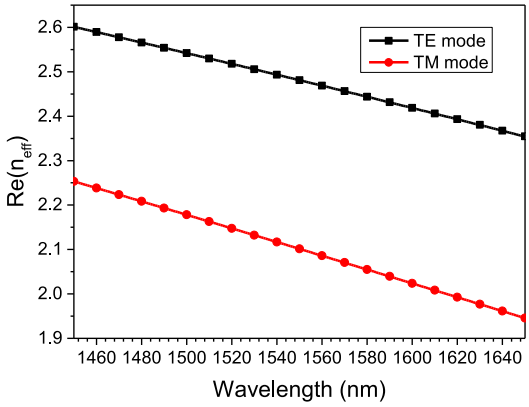

Fig. 6. Real part of effective modal index Re(n_{eff}) of graphene-silicon horizontal slot waveguide versus wavelength for TE and TM modes.

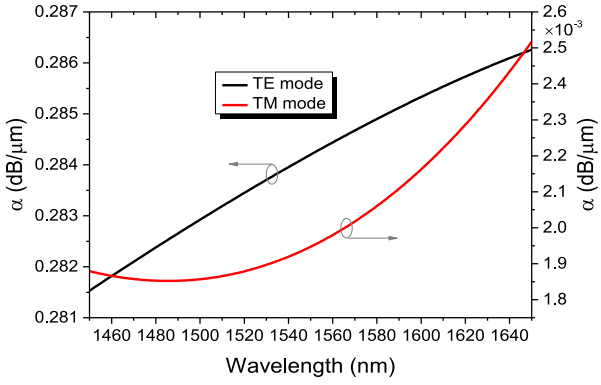

Fig. 7. Attenuation constant of TE and TM modes in graphene-silicon slot waveguide versus wavelength.

$\lambda = 1550$ nm for TM and TE modes is shown. In Fig. 5(a), one can see a rapid drop of loss due to the Pauli blocking effect for both modes (TE and TM). When the chemical potential of graphene is around 0 eV, it is interesting to note that the loss of the TE mode reaches its maximum value of $\sim$0.29 dB/μm, while the loss of the TM mode is only 0.019 dB/μm. This strong polarization dependent loss could be utilized to realize a compact polarizer. In the following simulations, we set the graphene's chemical potential $\mu = 0$ eV. We calculate the effective refractive indices Re(n_{eff}) of TM and TE modes in graphene-silicon horizontal slot waveguide. Fig. 6 depicts the real part of effective modal index Re(n_{eff}) of TM and TE modes.

The attenuation constant, known as the attenuation per unit length, is related to the imaginary part of the mode effective refractive index n_{eff} expressed by [18]

$$\alpha = \mathrm{Im}\,(n_{eff})\, k_0 \tag{3}$$

where Im(n_{eff}) is the imaginary part of the mode effective refractive index n_{eff}, and $k_0 = 17.372\pi/\lambda$ is the propagation constant at wavelength λ. The propagation loss is calculated by multiplying the attenuation constant and the waveguide length. Fig. 7 shows the attenuation constant (α) of TM and TE modes as a function of wavelength. The attenuation constant (α) is correlated with the imaginary part of the effective refractive index. One can clearly see from Fig. 7 that the attenuation of TE mode is almost one hundred times higher than TM mode, which is due to the considerably strong interaction between double-layer graphene sheets and TE mode in graphene-silicon horizontal slot waveguide.

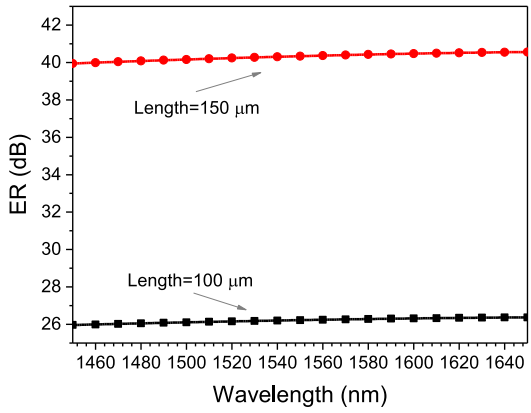

Fig. 8. Extinction ratio (ER) versus wavelength (1450 nm to 1650 nm) for graphene-silicon slot waveguide based polarizer with length = 100 μm and 150 μm.

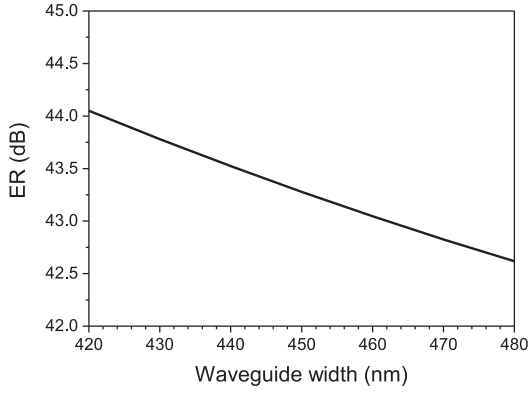

Fig. 9. Extinction ratio (ER) versus waveguide width for the graphene-silicon horizontal slot waveguide based polarizer. The incident light wavelength is 1550 nm, the chemical potential of graphene is 0 eV, and the waveguide length is 150 μm.

We evaluate the ER of graphene-silicon horizontal slot waveguide based polarizer. The ER of the graphene-assisted polarizer is defined by

$$\mathrm{ER} = 10\log_{10}\left(\frac{P_{TE}}{P_{TM}}\right) \tag{4}$$

where P_{TE} and P_{TM} are the output power of the TE mode and TM mode, respectively.

As shown in Fig. 8, the ER of a 100 μm long graphene-silicon slot waveguide based polarizer is higher than 26 dB when the wavelengths range from 1450 to 1650 nm, corresponding insertion loss less than 2 dB. Fig. 8 also shows that the ER of a 150 μm long graphene-silicon slot waveguide based polarizer is higher than 40 dB with insertion loss less than 3 dB, corresponding to wavelengths range from 1450 to 1650 nm. It is noted that the length of the designed graphene-assisted polarizer is much shorter than previously reported graphene based polarizers [18]–[20], while the ER is even higher, and the insertion loss is even less. Consequently, the graphene-silicon slot waveguide based polarizer shows superior operation performance and compatible with SOI platform.

We also analyze the fabrication error tolerance. In practical fabrication processes, the waveguide width, silicon and Si_3N_4 thicknesses of the graphene-silicon horizontal slot waveguide based polarizer might be slightly offset from their designed values. So it is valuable to comprehensively study the impacts of these possible practical fabrication imperfections on the operation performance of graphene-assisted polarizers. Fig. 9 shows the calculated ER as a function of the waveguide width

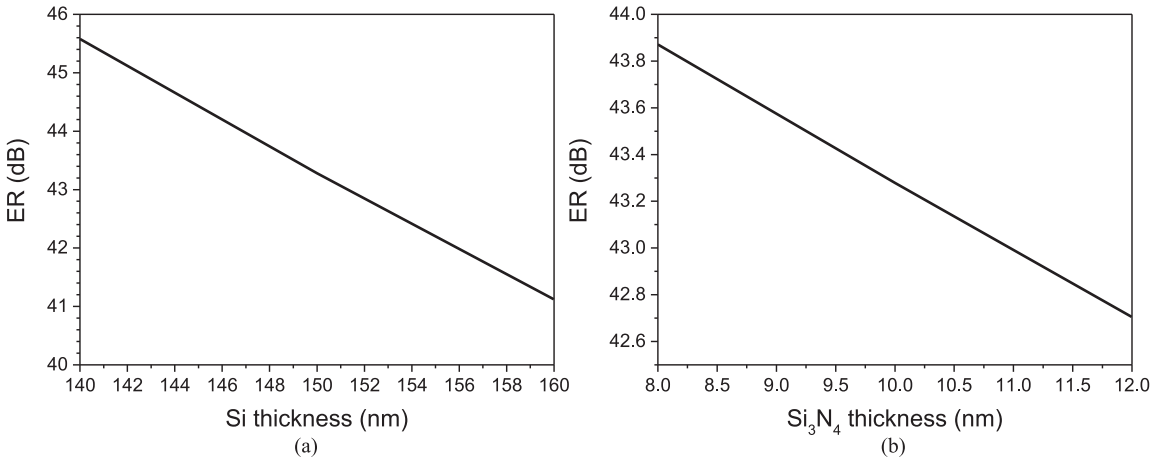

Fig. 10. Extinction ratio (ER) versus (a) Si thickness and (b) Si_3N_4 thickness for the graphene-silicon horizontal slot waveguide based polarizer. The incident light wavelength is 1550 nm, the chemical potential of graphene is 0 eV, and the waveguide length is 150 μm.

for the graphene-silicon horizontal slot waveguide based polarizer. The incident light wavelength is 1550 nm, the chemical potential of graphene is 0 eV, and the waveguide length is 150 μm. As shown in Fig. 9, the ER varies less than 3.4% (44.05 dB to 42.62 dB), when the waveguide width changes from 420 nm to 480 nm (i.e. $\pm$30 nm from 450 nm). In contrast, the ER is relatively sensitive to the change of the Si thickness. As shown in Fig. 10(a), the variation of the ER is less than 10.8% (45.58 dB to 41.12 dB) as the Si thickness has a $\pm$10 nm offset from 150 nm (140 nm to 160 nm). As shown in Fig. 10(b), the ER varies less than 2.7% (43.87 dB to 42.70 dB) as the Si_3N_4 thickness has a $\pm$2 nm offset from 10 nm (8 nm to 12 nm). The obtained results shown in Figs. 9 and 10 indicate favorable fabrication error tolerance of the designed graphene-assisted polarizer.

Remarkably, the total insertion loss of the TM mode is caused by two factors, i.e. coupling loss at the end of the polarizer and propagation loss suffered by the desired mode when passing through the polarizer. The coupling loss is due to the mismatch of mode profile between the hybrid waveguide (Si/graphene/Si_3N_4/graphene/Si) and input/output waveguides (Si/Si_3N_4/Si) as well as the reflection originated from the mode index mismatch between the hybrid waveguide and input/output waveguides. Actully, the mode profile in the hybrid waveguide is very similar to that in the input/output waveguides, and therefore, the loss induced by the mode profile mismatch is expected to be low. However, significant reflection might occur due to the mode index mismatch between the hybrid waveguide and input/output waveguides. One possible solution to solve this proplem is to use a taper section between the input/output waveguides and the hybrid waveguide [2], and thus the reflection and scattering losses between them could be suppressed. Another possible way to solve this proplem is to adopt a directional coupler in the lateral of the hybrid waveguide [25].

Additionally, the proposed graphene-silicon TM-pass polarizer might be fabricated following the similar fabrication process of silicon slot waveguide [26], [27] while incorporating the transfer of graphene. The possible fabrication process of the designed graphene-silicon TM-pass polarizer can be briefly described as follows. The Si waveguide can be fabricated by e-beam lithography (EBL) and inductively coupled plasma (ICP) etching process. A graphene sheet grown by chemical vapor deposition (CVD) is then mechanically transferred onto the Si waveguide. The growth of thin silicon nitride (Si_3N_4) layer can be realized by plasma enhanced chemical vapor deposition (PECVD) [28]. Another graphene sheet is mechanically transferred onto the Si_3N_4 layer. After that, a layer of amorphous silicon is deposited by PECVD or low pressure chemical vapor deposition (LPCVD) [29]. By EBL and ICP etching process the top waveguide is achievedd, which is finally covered by a SiO_2 cladding.

6. Conclusions

In summary, we present a design of compact graphene-assisted polarizers based on graphene-silicon slot waveguide structure with high extinction ratio, low insertion loss, broad bandwidth, small footprints, and compatible with SOI platform. When the double-layer graphene sheets are placed close to the slot region, its interaction with TE mode can be greatly enhanced. The selection of the device geometric parameters (waveguide width, silicon and Si_3N_4 thicknesses) is discussed. When the chemical potential of graphene is $\mu = 0$ eV, which does not need to be tuned by drive voltage, it is interesting to note that the loss of the TE mode reaches its maximum value of $\sim$0.29 dB/μm, while the loss of the TM mode is only $\sim$0.019 dB/μm. By employing a 150 μm long graphene-silicon slot waveguide based polarizer, the extinction ratio is higher than 40 dB and the insertion loss is less than 3 dB over 1450 to 1650 nm wavelength range. We also analyze the fabrication error tolerance and discuss the possible fabrication process of the designed graphene-silicon horizontal slot waveguide based polarizer.

References

[1] M. Z. Alam, J. S. Aitchison, and M. Mojahedi, "Compact and silicon-on-insulator-compatible hybrid plasmonic TE-pass polarizer," *Opt. Lett.*, vol. 37, no. 1, pp. 55–57, Jan. 2012.

[2] X. Sun, M. Z. Alam, S. J. Wagner, J. S. Aitchison, and M. Mojahedi, "Experimental demonstration of a hybrid plasmonic transverse electric pass polarizer for a silicon-on-insulator platform," *Opt. Lett.*, vol. 37, no. 23, pp. 4814–4816, Dec. 2012.

[3] M. Z. Alam, J. S. Aitchsion, and M. Mojahedi, "Compact hybrid TM-pass polarizer for silicon-on-insulator platform," *Appl. Opt.*, vol. 50, no. 15, pp. 2294–2298, May 2011.

[4] J. Zhang, E. Cassan, and X. Zhang, "Wideband and compact TE-pass/TM-stop polarizer based on a hybrid plasmonic Bragg grating for silicon photonics," *J. Lightw. Technol.*, vol. 32, no. 7, pp. 1383–1386, Apr. 2014.

[5] C. H. Chen, L. Pang, C. H. Tsai, U. Levy, and Y. Fainman, "Compact and integrated TM-pass waveguide polarizer," *Opt. Exp.*, vol. 13, no. 14, pp. 5347–5352, Jun. 2005.

[6] K. S. Novoselov *et al.*, "Electric field effect in atomically thin carbon films," *Science*, vol. 306, no. 5696, pp. 666–669, Oct. 2004.

[7] A. K. Geim and K. S. Novoselov, "The rise of graphene," *Nature Mater.*, vol. 6, no. 3, pp. 183–191, Mar. 2007.

[8] F. Schwierz, "Graphene transistors," *Nature Nanotechnol.*, vol. 5, no. 7, pp. 487–496, May 2010.

[9] F. Bonaccorso, Z. Sun, T. Hasan, and A. C. Ferrari, "Graphene photonics and optoelectronics," *Nature Photon.*, vol. 4, no. 9, pp. 611–622, 2010.

[10] L. Liao *et al.*, "High-speed graphene transistors with a self-aligned nanowire gate," *Nature*, vol. 467, no. 7313, pp. 305–308, Sep. 2010.

[11] M. Liu *et al.*, "A graphene-based broadband optical modulator," *Nature*, vol. 474, no. 7349, pp. 64–67, May 2011.

[12] M. Liu, X. Yin, and X. Zhang, "Double-layer graphene optical modulator," *Nano Lett.*, vol. 12, no. 3, pp. 1482–1485, Feb. 2012.

[13] Y. Ding *et al.*, "Effective electro-optical modulation with high extinction ratio by a graphene–silicon microring resonator," *Nano Lett.*, vol. 15, no. 7, pp. 4393–4400, Jun. 2015.

[14] C. T. Phare, Y. H. D. Lee, J. Cardenas, and M. Lipson, "Graphene electro-optic modulator with 30 GHz bandwidth," *Nature Photon.*, vol. 9, no. 8, pp. 511–514, Jul. 2015.

[15] T. Sohier and B. Yu, "Ultralow-voltage design of graphene PN junction quantum reflective switch transistor," *Appl. Phys. Lett.*, vol. 98, no. 21, May 2011, Art. no. 213104.

[16] L. Wu, H. S. Chu, W. S. Koh, and E. P. Li, "Highly sensitive graphene biosensors based on surface plasmon resonance," *Opt. Exp.*, vol. 18, no. 14, pp. 14395–14400, Sep. 2010.

[17] F. Xia, T. Mueller, Y. Lin, A. Valdes-Garcia, and P. Avouris, "Ultrafast graphene photodetector," *Nature Nanotechnol.*, vol. 4, no. 12, pp. 839–843, Oct. 2009.

[18] C. Guan, S. Li, Y. Shen, T. Yuan, J. Yang, and L. Yuan, "Graphene-coated surface core fiber polarizer," *J. Lightw. Technol.*, vol. 33, no. 2, pp. 349–353, Jan. 2015.

[19] J. T. Kim and C. G. Choi, "Graphene-based polymer waveguide polarizer," *Opt. Exp.*, vol. 20, no. 4, pp. 3556–3562, May 2012.

[20] C. Pei *et al.*, "Broadband graphene/glass hybrid waveguide polarizer," *IEEE Photon. Technol. Lett.*, vol. 27, no. 9, pp. 927–930, May 2015.

[21] X. Yin, T. Zhang, L. Chen, and X. Li, "Ultra-compact TE-pass polarizer with graphene multilayer embedded in a silicon slot waveguide," *Opt. Lett.*, vol. 40, no. 8, pp. 1733–1736, Sep. 2015.

[22] M. S. Kwon, "Discussion of the epsilon-near-zero effect of graphene in a horizontal slot waveguide," *IEEE Photon. J.*, vol. 6, no. 3, pp. 1–9, Jun. 2014.

[23] R. E. de Oliveira and C. J. de Matos, "Graphene based waveguide polarizers: In-depth physical analysis and relevant parameters," *Sci. Rep.* vol. 5, pp. 1–6, Jan. 2015.

[24] M. Bass, E. W. V. Stryland, D. R. Williams, and W. L. Wolfe, *Handbook of Optics*, 3rd ed. New York, NY, USA: McGraw-Hill, 2009, ch. 4.

[25] J. S. Shin and J. T. Kim, "Broadband silicon optical modulator using a graphene-integrated hybrid plasmonic waveguide," *Nanotechno.*, vol. 26, no. 36, Aug. 2015, Art. no. 365201.
[26] K. Preston and M. Lipson, "Slot waveguides with polycrystalline silicon for electrical injection," *Opt. Exp.*, vol. 17, no. 3, pp. 1527–1534, Jan. 2009.
[27] J. V. Galan *et al.*, "Silicon sandwiched slot waveguide grating couplers," *Electron. Lett.*, vol. 45, no. 5, pp. 262–263, Feb. 2009.
[28] L. Zhao *et al.*, "Low-temperature growth of thin silicon nitride film by electron cyclotron resonance plasma irradiation," *Jpn. J. Appl. Phys.*, vol. 43, no. 1A-B, pp. L47–L49, Dec. 2003.
[29] H. Dalir, Y. Xia, Y. Wang, and X. Zhang, "Athermal Broadband graphene optical modulator with 35 GHz speed," *ACS Photon.*, vol. 3, no. 9, pp. 1564–1568, Jun. 2016.